Bulletin of the Seismological Society of America, Vol. 92, No. 7, pp. 2689–2703, October 2002

Evidence for Two Surface Ruptures in the Past 500 Years on the San Andreas Fault at Frazier Mountain, California

by Scott C. Lindvall, Thomas K. Rockwell, Timothy E. Dawson, John G. Helms, and Kristin Weaver Bowman

Abstract We conducted paleoseismic studies in a closed depression along the San Andreas fault on the north flank of Frazier Mountain near Frazier Park, California. We recognized two earthquake ruptures in our trench exposure and interpreted the most recent rupture, event 1, to represent the historical 1857 earthquake. We also exposed evidence of an earlier surface rupture, event 2, along an older group of faults that did not rerupture during event 1. Radiocarbon dating of the stratigraphy above and below the earlier event constrains its probable age to between A.D. 1460 and 1600. Because we documented continuous, unfaulted stratigraphy between the earlier event horizon and the youngest event horizon in the portion of the fault zone exposed, we infer event 2 to be the penultimate event. We observed no direct evidence of an 1812 earthquake in our exposures. However, we cannot preclude the presence of this event at our site due to limited age control in the upper part of the section and the possibility of other fault strands beyond the limits of our exposures. Based on overlapping age ranges, event 2 at Frazier Mountain may correlate with event B at the Bidart fan site in the Carrizo Plain to the northwest and events V and W4 at Pallett Creek and Wrightwood, respectively, to the southeast. If the events recognized at these multiple sites resulted from the same surface rupture, then it appears that the San Andreas fault has repeatedly failed in large ruptures similar in extent to 1857.

Introduction

The dextral strike-slip San Andreas fault in southern California is one of the most studied faults in the world, yet due to the relatively short historical period in California, a direct record of past large earthquakes along the fault is lacking. Consequently, paleoseismology is the primary means used to augment the short historical record and derive a record of paleoearthquakes along the San Andreas fault. Knowledge of the timing, location, and slip distribution of past earthquakes is critical to understand the long-term behavior of the San Andreas fault and to forecast future large earthquakes.

A number of well-studied paleoseismic sites have been developed along the San Andreas fault southeast of Pallett Creek; however, very little data exists for the Big Bend region of the fault (Fig. 1). Except for the San Emigdio trench site near Mil Potrero (Davis, 1983), there are no dated paleoseismic records along the 200-km reach of the fault between Pallett Creek and the Bidart Fan site in the Carrizo Plain (Fig. 1). Given the paucity of data in the Big Bend region of the fault, we focused our search for potential paleoseismic sites along the portion of the San Andreas fault between Mil Potrero and Three Points, with the objective of finding a site that would yield a record of the past several prehistoric earthquakes. Specifically, we were looking for a location on the fault that contained a continuous sedimentary record and abundant detrital charcoal or layers of peat to provide age control. Closed depressions, or sags, commonly offer such conditions because they serve as low energy depocenters for fine-grained material. Sediments in these environments may be deposited frequently (often seasonally), and typically they contain abundant organic and plant material.

In this article, we present new paleoseismic results from the Frazier Mountain site located midway between Pallett Creek and Bidart Fan (Fig. 1). The Frazier Mountain site is a closed depression located on the Mesa Valley Farm property along the northern flank of Frazier Mountain, between the towns of Frazier Park and Gorman (Fig. 2). The trench site is 2 km west of Tejon Pass near the intersection of the Garlock and San Andreas fault zones. Although high groundwater conditions from the near-record El Niño rainfall of 1998 prevented us from obtaining a long paleoseismic record at Frazier Mountain, the site does provide new data in a critical area and helps provide constraints on a prehistoric large rupture near Fort Tejon.

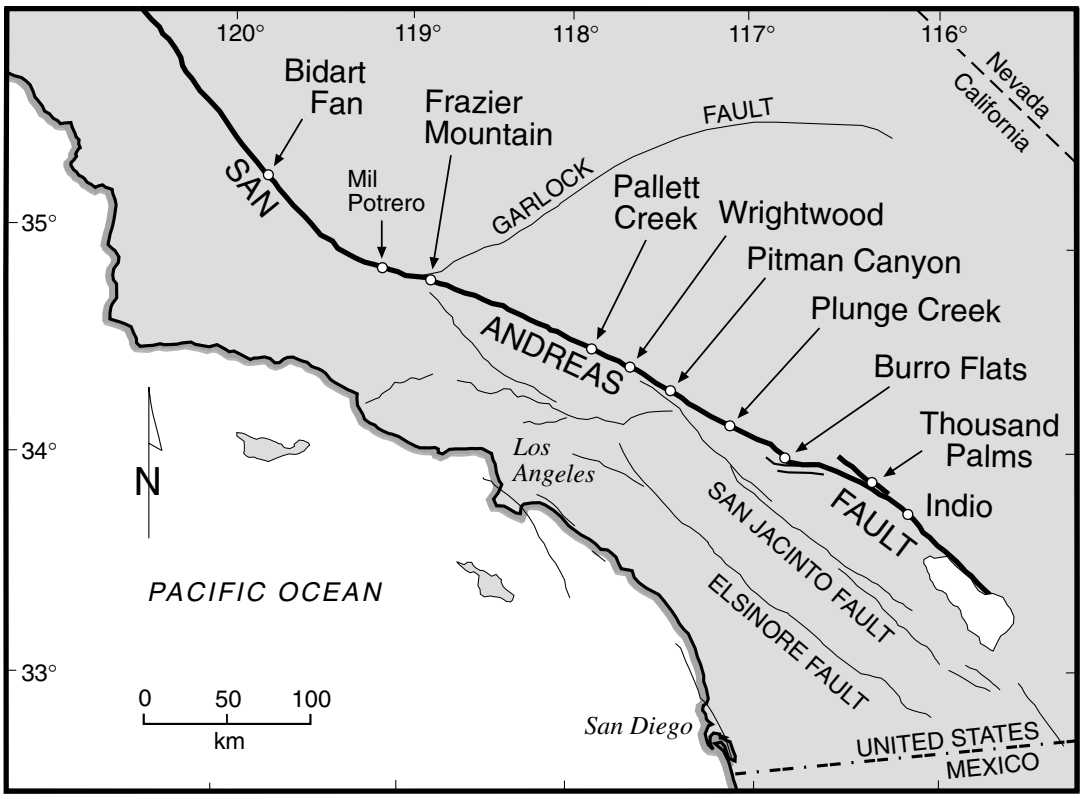

Figure 1. Location of the Frazier Mountain study site with respect to other paleoseismic sites (white dots) along the southern San Andreas fault zone.

Geologic and Geomorphic Setting

The closed depression at the Frazier Mountain site is located in a minor right step in the San Andreas fault zone (Fig. 3). A primary strand of the fault has produced an uphill-facing scarp, with a maximum height of ~6 m, along the northern margin of the closed depression (Fig. 3a, 4). At the site, the San Andreas fault zone separates dissected, older alluvium on the north from nonmarine, white sandstone of the Pliocene Hungry Valley Formation (Crowell, 1952; Duebendorfer, 1979) on the south (Fig. 3b). The combination of a local north-side-up component of slip and the juxtaposition of locally higher topography on the north side of the fault has blocked a relatively large drainage west of the site and trapped late Holocene alluvium within the lower topography along the fault zone (Fig. 3b). The older alluvium north of the fault, which exhibits dissected surfaces and contains abundant cobbles and boulders, has been mapped by several workers and assigned ages ranging from middle Holocene to Pleistocene (Qof of Duebendorfer, 1979; Qoa2 of Davis, 1983; and Q3 of Zhou *et al.*, 1991). In this article, we refer to these deposits as simply older alluvium, because (1) we have not directly dated these deposits and (2) they appear significantly older than the latest Holocene deposits in the closed depression, which were the focus of our study.

Active alluvial fans bound the eastern and western margins of the site and represent the primary sediment sources for the closed depression, which is inundated with standing water in wet years (Fig. 3, 4). Late Holocene alluvium originating from the blocked drainage west of the site (Fig. 3b) forms a relatively steep gradient into the closed depression and appears to form an eastward-prograding alluvial fan confined to the margins of the fault zone (Fig. 4). The depth of the basin has been further enhanced by a small alluvial fan that blocks a potential drainage outflow east of the closed depression (Fig. 4). The small eastern fan is composed almost exclusively of sands derived from Hungry Valley Formation sandstone, whereas the larger western fan contains a major component of sand and gravel derived from the Precambrian gneisses of Frazier Mountain.

We mapped several fault strands across the site based primarily on geomorphic observations and trench exposures (Fig. 4, 5). The northern strand forms a ~6-m-high scarp along the northern margin of the closed depression (Fig. 5). A portion of this fault was poorly expressed in massive, highly bioturbated deposits at the northern end of our trench. A few meters south of the northern fault, a small zone of buried faults was exposed in our 1997 excavation (Fig. 4).

A central fault strand is shown bifurcating westward from the northern fault into the central portion of the closed depression (Fig. 4). This central strand is expressed as a small (20–30 cm) north-facing scarp near the toe of the small alluvial fan. The central fault, which also exhibits a subtle

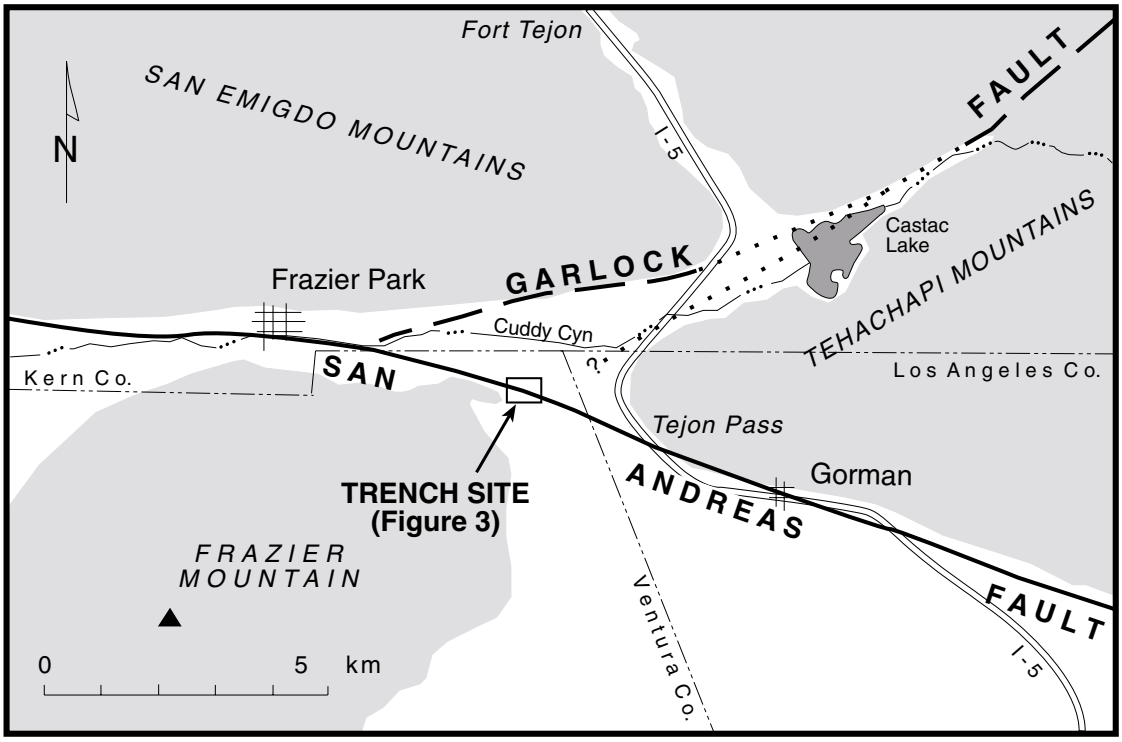

Figure 2. Map of the greater study site area near the intersection of the Garlock and San Andreas faults. The trench site (rectangle) is located on the northwest flank of Frazier Mountain (triangle) between the towns of Frazier Park and Gorman and west of Interstate 5 (I-5). Mountainous terrain underlain by crystalline rock shown in gray; lower elevations and valleys underlain by Pliocene Hungry Valley Formation and Pleistocene–Holocene alluvium shown in white.

vegetation lineament, is interpreted to branch westward into a northwest-striking fault and a westerly continuation of the central strand. The northwest-striking fault forms a pronounced groundwater barrier and was encountered in our 1999 trench exposure near the dead tree (Fig. 4). The westward continuation of the central fault south of the 1999 trench is somewhat speculative and was inferred based on the linear contours of the ground surface and the equivocal expression of a subtle scarp (~10 cm).

A southern strand is inferred along the southern margin of the depression nearly coincident with the base of the steep bedrock slopes (Fig. 3, 4). The inferred southern fault is located south of our trench exposures and is not expressed geomorphically in the young alluvium. North of the main fault zone, a series of east-northeast-striking, secondary faults are mapped within the older alluvium (Fig. 3b). This pattern of faulting may represent complexities related to the intersection of the Garlock fault zone.

The geometry of the faults within the closed depression suggests that the sag may have formed largely as a pull-apart basin or rhomboid graben within a right step-over. The northwest-striking fault within the closed depression and the northwesterly striking portion of the northern fault at the northeastern margin of the closed depression may represent the eastern and western margins of a subsiding block. However, we realize that there may be additional unrecognized, buried faults within the closed depression beyond the limits of our excavations. East and west of the closed depression the fault zone appears to exhibit a more simple, linear trace. About 200 m east of the trench site, an incised drainage is sharply deflected 75 m, illustrating that deformation is focused along a narrow zone of faulting (Fig. 3).

The most recent surface rupture through the Frazier Mountain site was the historical Fort Tejon earthquake of 9 January 1857, which broke over 350 km of the San Andreas fault from Cholame Valley to Cajon Pass (Sieh, 1978). In the vicinity of the Frazier Mountain site, dextral displacements from the 1857 Fort Tejon earthquake were on the order of ~6 m, based on measurement of offset geomorphic features (Sieh, 1978).

Site History and Methods

We first excavated several backhoe test pits in 1997 to locate good stratigraphy, and an exploratory trench was placed at the base of the northern scarp (Fig. 4). This initial exploratory trench exposed a 2.5-m-deep section of unsaturated, well-stratified distal fan and pond deposits. Walls of the trench were scraped clean and gridded with string on the west wall. The grid cell dimensions were 0.5 m in height

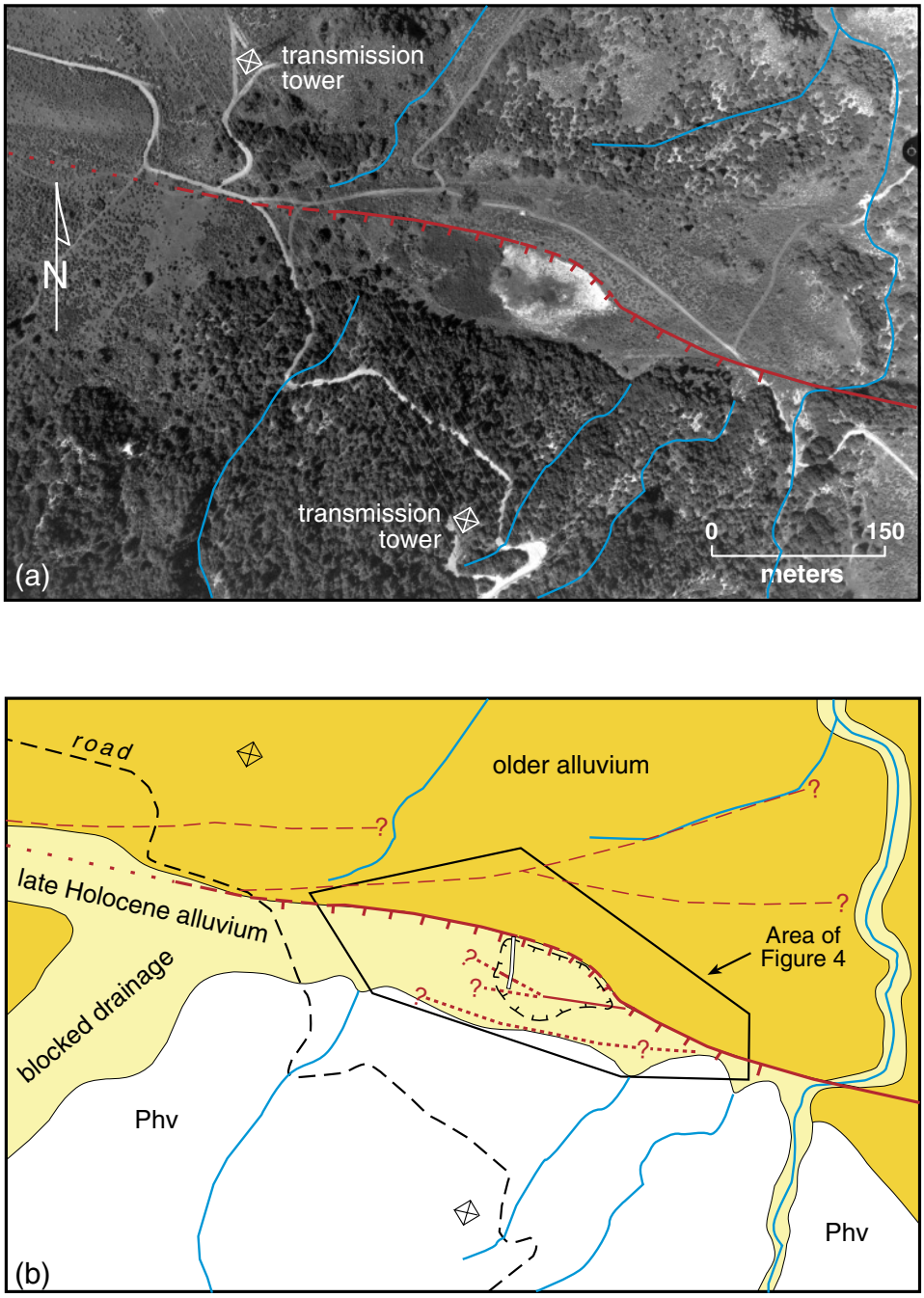

Figure 3. Aerial view and geologic map of the Frazier Mountain site. (a) 1996 air photo of the closed depression showing the prominent scarp-forming strand (red), drainages (blue), and towers of the power transmission lines west of the closed depression. The recently inundated area appears as lighter color. (b) Generalized geologic map of the same area in (a) showing faults (red), drainages (blue), late Holocene alluvium (yellow), older alluvium (orange), and Pliocene Hungry Valley Formation (white). Location of the trench is shown as a white rectangle and the area frequently inundated is outlined in black dashed line with tic marks.

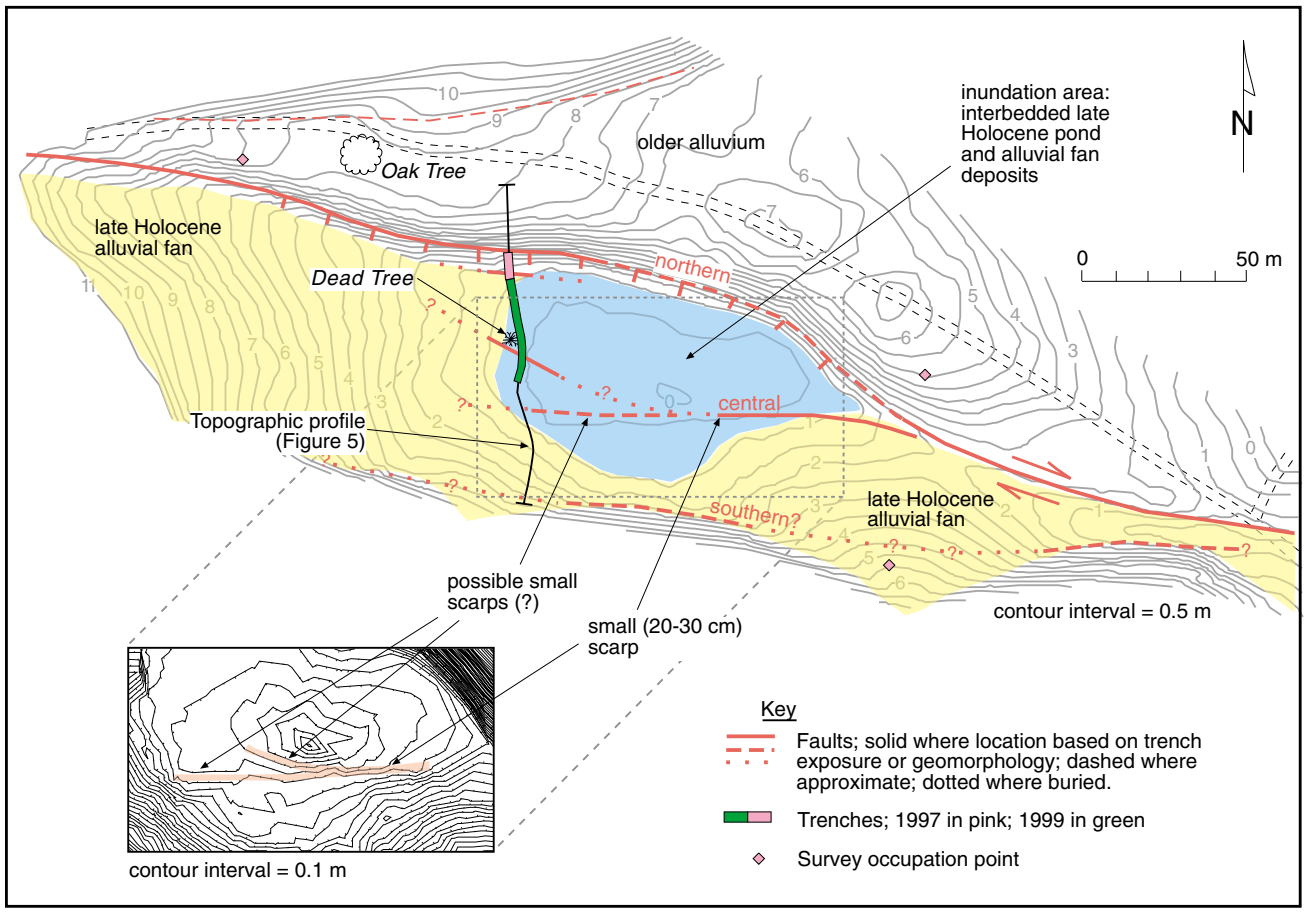

Figure 4. Detailed topographic and geologic map of the Frazier Mountain site showing locations of faults, trenches, surveyed topographic profile, and the distribution of late Holocene alluvial fan deposits (yellow). Blue area indicates approximate extent of inundation during the spring of 1998. Pink diamonds mark survey occupation points. Inset map shows higher resolution topography (10-cm contour interval) within the pond where subtle topographic scarps are interpreted as faults.

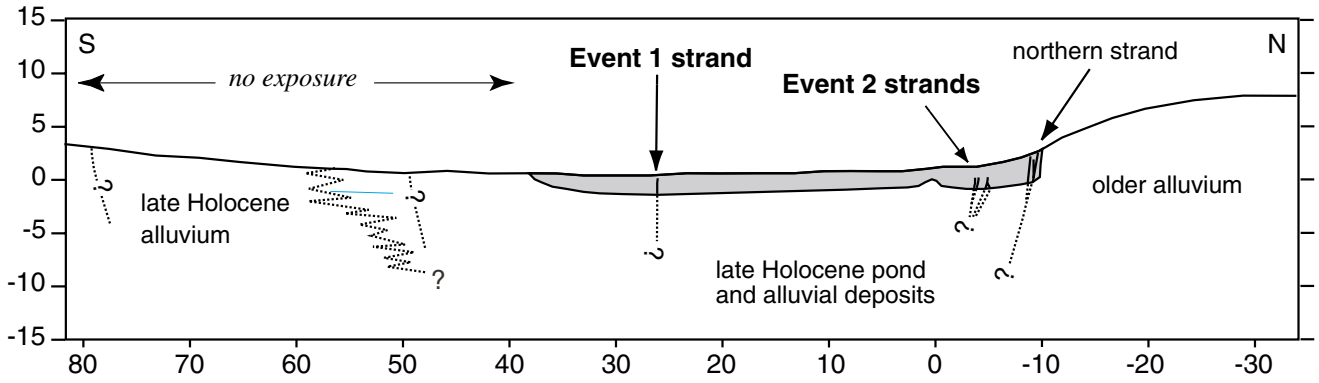

Figure 5. Topographic profile and schematic cross section along the axis of the trench showing scarp morphology, distribution of geologic materials, trench (gray), fault strands encountered in the trench, and faults mapped beyond the southern limit of our trench exposure. Horizontal distance and relative elevation shown in meters.

and 1.0 m in length in order to accommodate the dimensions of the camera-mounted frame used for photographing the trench wall. Faults and contacts were etched into the wall to enhance their visibility in the photographs. Over 50 radiocarbon samples were collected from the walls of the trench. The samples were flagged and labeled so we could later identify each sample location in the photographs. Finally, the west wall of the trench was photographed, cell by cell, using a 20-mm rectilinear lens to minimize distortion. Hydraulic shores were moved, and the walls were locally cleaned in order to provide a complete unobstructed view of the entire trench wall. Photographs were later scanned and electronically tiled together to produce a complete photomosaic of the west wall of the trench. The geologic interpretation was then drawn on the mosaic, following the field interpretation as sketched on the trench face.

About 25–30 m south of the 1997 exploratory trench, we excavated a test pit and encountered groundwater at a depth of only 1.4 m. The locally high groundwater convinced us to postpone extending the trench across the groundwater barrier near the dead tree (Fig. 4) until we had the means to lower the water table. However, following the 1997–1998 El Niño winter season, the closed depression was inundated with up to 1.2 m of standing water as late as June 1998. The resulting pond and saturated ground conditions prevented trench excavations during 1998, and therefore, efforts concentrated instead on (1) site mapping, (2) radiocarbon dating, (3) interpretation and analysis of our 1997 exploratory trench, and (4) monitoring the receding water levels. During the winter, spring, and summer of 1999, the pond evaporated and the depth to groundwater fell to about 1 m below the ground surface. In September 1999, we began extending the 1997 trench southward, during two stages of excavation, for an additional 35 m of exposure (Fig. 4). Water was pumped from the trench, resulting in a gradual lowering of the water table. By reopening the southernmost end of the 1997 trench, we were able to locate and, therefore, accurately tie into the existing string grid and maintain the same vertical and horizontal stationing between the 1997 and 1999 excavations. This allowed us to extend the same radiometrically dated stratigraphic section across the entire length of trench, which totals greater than 45 m (Figs. 4, 5).

The walls of the 1999 trench were cleaned, and the stratigraphic contacts and faults were etched and marked with painted nails. The west wall was gridded and logged at a scale of 1 inch = 50 cm. We decided not to use the photo logging method on the 1999 exposure because we could not move the shores without risking local slumping of the trench walls.

Stratigraphy

The stratigraphy exposed in the trench generally consists of bedded silt, sand, and clayey silt with unit thicknesses ranging from about 5 cm on some individual beds to about 50 cm for more massive undifferentiated packages. The majority of the deposits are laterally continuous and can be traced the entire length of the trench (Fig. 6). Strata within the pond slope gently down to the south from the north margin (station −10 m) to the structural low or center of the pond (station +20 m). Continuing southward of the center of the pond, the strata slope gently up between station +20 m and +35 m (Fig. 6).

We labeled units numerically from 1 to 14 (Figs. 7, 8) from the youngest to oldest, respectively. Because we reexcavated a small portion of the 1997 trench, we could directly correlate individual units and packages of units between these two sections of the trench (Fig. 6). Descriptions of the stratigraphic units are provided in Table 1.

The two most prominent marker beds that exhibited sharp upper and lower contacts were units 3 and 6 (Fig. 4). Unit 3 is a well-sorted, fine-grained sand that grades southward into two separate subunits, a well-sorted, fine grained sand (unit 3b) and an overlying unit of poorly sorted, silty fine to coarse sand with fine gravel (unit 3a). We interpret this sandy package to represent distal alluvial fan deposits prograding eastward into the pond (Fig. 4). Unit 3 also represents the stratigraphically highest unit that is completely faulted by the youngest event recognized in our trench (Figs. 4, 6). Unit 6, which lies about 1 m below unit 3, is a distinct deposit of clayey silt locally grading to clayey sand that contains common angular silt nodules and is interpreted to represent a period of pond deposition.

Evidence of Faulting

The trench exposed three zones of brittle faulting (Fig. 5). The northernmost zone, located at station −10 m, was weakly expressed in the massive older alluvial deposits (Qoa) as a diffuse zone of shears near the base of the steep scarp that forms the northern margin of the closed depression (Fig. 6). It is not clear whether the entire width of the northern, pond-bounding fault zone was exposed. The second zone of faulting was exposed between stations −2 m and −5 m and appears to represent a zone of minor slip (Figs. 6, 7). The third and southernmost zone of exposed faulting consisted of a single major fault near station +26 m that exhibits about 30 cm of apparent vertical separation and mismatches in most strata (Figs. 6, 8). In addition to brittle faulting, we observed evidence of liquefaction in the form of sand blows near stations +17 m and +26 m (Fig. 8). The combination of brittle slip across faults and the nonbrittle liquefaction-related features and deposits in the trench provide structural and stratigraphic evidence for two earthquake ruptures within our trench exposure. Several key stratigraphic units exposed in the exploratory trench were correlated across the fault zone and were used for event identification.

Event 1

The youngest earthquake recognized in our trenches is referred to as event 1. The strongest evidence for this event

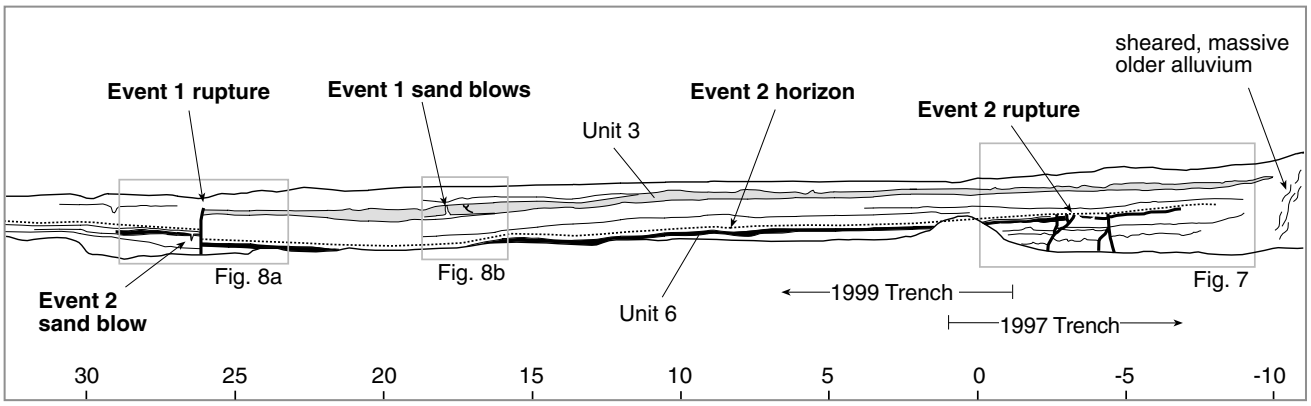

Figure 6. West view of the west wall composite log of the trench exposure excavated in 1997 and 1999 showing continuity of stratigraphic section across trench south of the fault bounding the northern margin of the pond. This northern fault strand, which is associated with the greatest geomorphic expression and presumably ruptured in 1857, was poorly expressed as a sheared zone within the massive gravelly sands of the older alluvial deposits. The sand of unit 3 (gray) and overlying strata are interpreted to represent alluvial fan prograding eastward into the pond. Strata below unit 3 generally contain larger components of silt and clay, which suggest a greater percentage of water-laid deposits. Horizontal distance shown in meters, no vertical exaggeration.

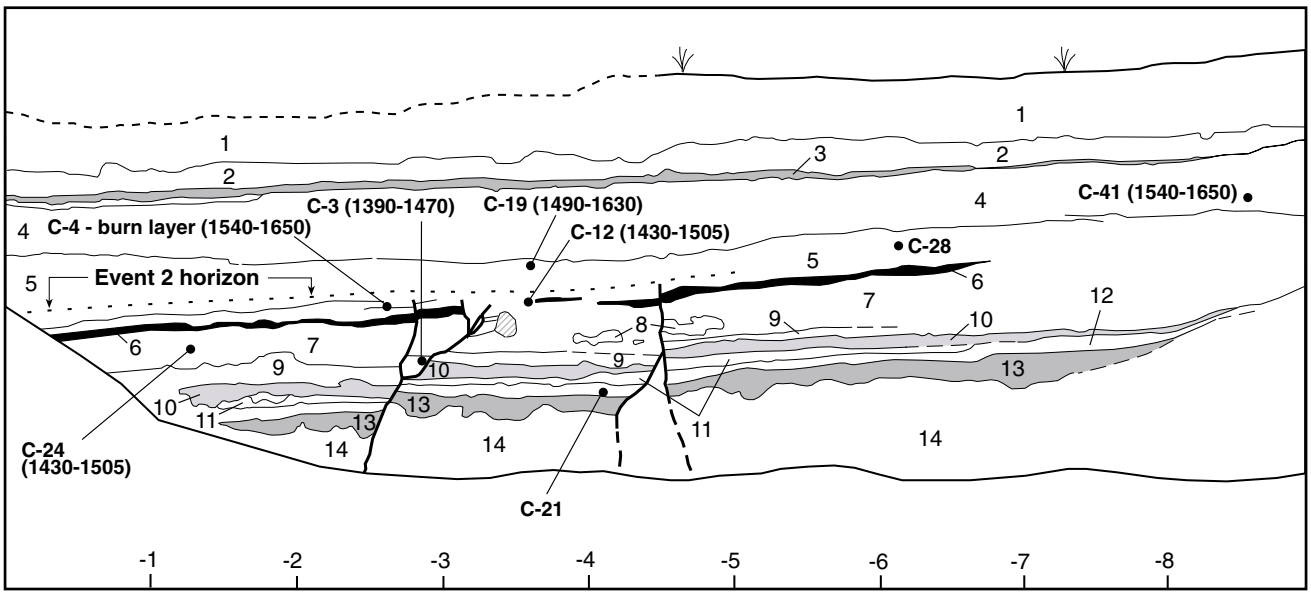

Figure 7. Log of the 1997 portion of the trench where evidence was found for event 2, an earthquake that occurred between about A.D. 1460 and A.D. 1600. The approximate position of event 2 horizon is shown as a dotted line within unit 5. Fault strands were observed cutting unit 6 and into the lower portion of unit 5. The overlying contact between units 4 and 5 was not offset; therefore, we interpret that event 2 occurred during the deposition of unit 5. Dated charcoal samples are shown with their 2σ stratigraphically ordered age ranges determined using the program OxCal (Ramsey, 1995, 2000). Light gray cross-hatched areas represent large krotovina.

is the upward termination of the northwest-striking fault strand that traverses the center of the pond near station +26 m (Figs. 6, 8a). The fault, which strikes N61 °W across the trench, exhibits about 30 cm of apparent vertical separation of unit 6c and evidence of horizontal slip in the form of mismatched stratigraphic units across a narrow (3–5 cm) zone (Fig. 8a). This fault is terminated by unbroken strata of units 1 and 2. These units are combined on Figure 8 because of their massive character in the vicinity of the fault.

We also observed irregular-shaped bodies of well-

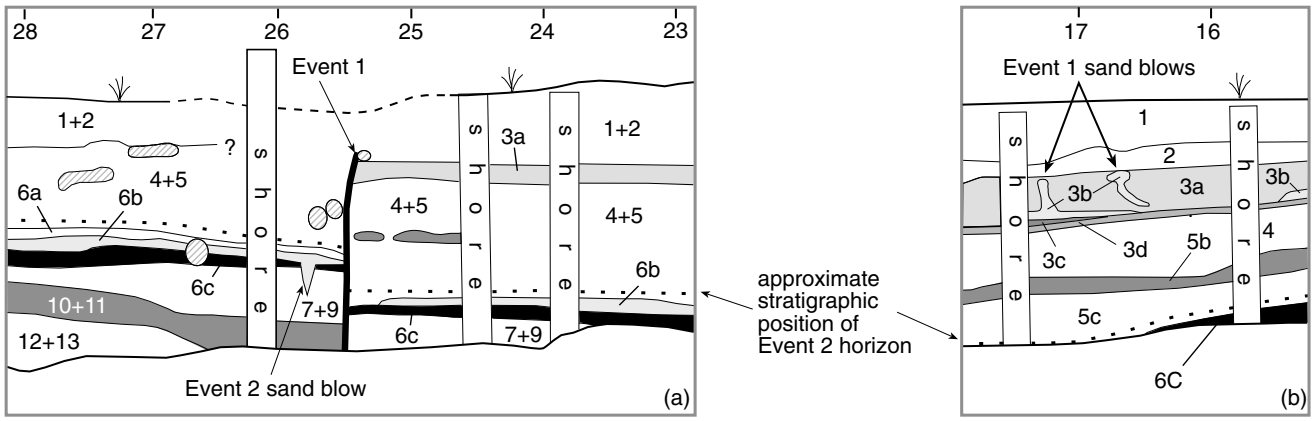

Figure 8. Detailed areas (a) and (b) from Figure 6 that show evidence for the most recent earthquake, event 1, which we interpret as the 1857 earthquake. In detail (a), a single fault cuts to within about 35–40 cm of the ground surface and vertically displaces the strata containing the event 2 horizon (dotted line) by approximately 30 cm. Because unit 3a is not present south of this strand, we do not have a direct measurement of the vertical displacement in event 1 and therefore, we can only assume that the ~30 cm of apparent vertical slip represents cumulative displacement from both earthquakes. Light gray cross-hatched areas represent large krotovina. Detail (b) shows two sand blows that reach the top of unit 3a, which is the same event horizon as the upward termination of the fault shown in (a). Based on their similar stratigraphic position, we interpret that both the upward termination of the fault and the sand blows are evidence for event 1.

Table 1
Unit Descriptions from Trench Exposures in 1997 and 1999

Unit Numbers		Description
1997	1999	
1	1	Sandy silt; brown (10YR4/3; w) fine grained, moderately sorted, moderately indurated with common to many roots, localized mottling; diffuse boundary with unit 2
2	2	Silty sand; dark brown (10YR3/3; w) fine to coarse grained, poorly sorted, with orange (iron oxide) mottles and common roots; coarsens northward to include fine gravel; fines upward and has abrupt lower contact
na	3a	Silty sand; dark brown, poorly sorted, with few granules
3	3b	Sand; dark yellowish brown (10YR3/4; w) fine grained, well sorted with orange (iron oxide) mottles and common roots and krotovina; abrupt lower contact with unit 4 at the northern end of the trench
na	3c	Silt; gray-tan
na	3d	Silt; tan with common thin organic lamination at base of unit
4	4	Sandy silt; dark brown (10YR3/3; w) fine-to very fine-grained, well sorted with common roots, localized oxidation and a gradational and wavy lower contact; top of unit is organic rich
5	5a	Sandy silt; brown (10YR4/3; w) clayey fine-grained, well-sorted sand with a gradational lower contact
5	5b	Sand; dark brown (10YR3/3; w) silty, fine grained, with a thin, intermittent organic (peat) layer at its base; few to common krotovina, common orange (iron oxide) mottles, few to common roots and a sharp lower contact
5	5c	Sandy silt; brown (10YR4/3; w) fine-grained, well-sorted sand with few roots and a sharp lower contact
na	6a	Silt; medium brown with nodules; lighter in color than unit below
na	6b	Silty sand; light to medium brown, fine grained
6	6c	Clayey silt to clayey sand; brown (10YR4/3; w) clayey silt grading to very fine-grained clayey sand; well sorted with common angular, granule-sized silt nodules cemented by iron and manganese oxide
7 + 8 + 9	7 + 9	Clayey silt to clayey sandy silt; dark brown (10YR3/3; w) clayey silt to very fine-grained clayey sandy silt; well sorted with common angular, granule-sized silt nodules cemented by iron and manganese oxide
10	10	Sandy silt; very dark brown (10YR3/2; w) very fine grained, with minor clay, darker than above and below
11	11	Sandy clayey silt; very dark brown (10YR3/2; w), appears lighter in color than unit above
12 + 13	12 + 13	Sandy silt; very dark brown (10YR3/2; w) fine grained with minor medium-grained sand

sorted, fine sand (unit 3b) that extend from a discontinuous layer of unit 3b upward to the top of unit 3a near station +17 m. We interpret these features to represent small dikes of liquefied sand that formed in an event (event 1) following the deposition of unit 3a and prior to deposition of unit 2 (Figs. 6, 8). The fault tip at station +26 m and the liquefaction features at station +17 m all terminate at the same stratigraphic level, which lies between about 40 and 60 cm below the ground surface (Fig. 8).

The fault at station +26 m exhibits a south-side-up component of slip, which is similar to the sense of vertical separation suggested by the small (20–30 cm) north-facing scarp on the central strand to the east. Note, however, that there is no discernable scarp preserved in the ground surface at the trench (Fig. 8). The lack of a scarp at the trench can be explained by one or more of the following processes: (1) a decreasing vertical component of slip westward through the pond, (2) burial of the scarp by eastward-prograding fan deposits, or (3) erosion of the scarp (and removal of unit 3) south of the fault. We consider erosion highly unlikely within a closed depression and prefer both a westward decrease in vertical slip and burial of the scarp to explain the stratigraphy and subtle geomorphology at the site. The absence of unit 3 south of the fault is likely the result of significant dextral slip that juxtaposed a thicker, more proximal section (containing unit 3) north of the fault against a thinner, more distal section (in which unit 3 was never deposited) south of the fault. The emergence of this fault strand as a surface scarp ~30 m to the east of our trench, along with the observation that this is the youngest recognized surface rupture at this site, lead us to conclude that this resulted from the historical Fort Tejon earthquake of 9 January 1857.

The fault strand along the northern margin of the sag, which we interpret as a significant fault because it forms a ~6-m-high scarp and defines the edge of the depression, was expressed as a broad zone of shearing in relatively massive, conglomeratic colluvium. Bioturbation has all but erased the expression of the fault in the upper portions of the trench exposure, probably because that part of the section generally remains above the water table. Thus, we were not able to resolve whether this northern strand ruptured in the 1857 earthquake, although we consider it likely because it is the only continuous fault expressed geomorphically west of the pond.

Event 2

Evidence for an earlier earthquake, event 2, is expressed in the trench as two fault strands between stations −2 and −5 m that terminate within unit 5 (Figs. 6, 7). This event horizon is located approximately 1.3 m below the present ground surface, much deeper than that of event 1. These two small zones of faulting contain anastomosing and bifurcating splays that result in four individual fault tips terminating at the same stratigraphic position (Fig. 7). Although upward termination of faults can be tenuous evidence for an event, as observed by Fumal *et al.* (1993), the faults exposed in this trench consistently terminate at the same stratigraphic horizon, which allows for a higher degree of confidence in making this assertion.

The minor faults that provide evidence for event 2 are probably subsidiary strands to the northern fault strand and may have only minor displacements, but nevertheless exhibit evidence of lateral slip. Individual strata are mismatched across the fault strands, and therefore, we are reasonably confident that the faults are directly accommodating a portion of the total right-lateral shear across the fault zone and are not related to the settling of sediments toward the center of the depression due to shaking. This issue is important because if the faults were the result of settling alone, events identified along them may not be the result of slip on the San Andreas fault. Conceivably, an earthquake along the Garlock fault, which intersects the San Andreas fault near Frazier Park, could cause shaking-induced settling at the Frazier Mountain site. Although the amount of lateral shear could not be quantified in the trench, the evidence for lateral slip precludes the possibility that these features are the result of merely settlement during strong ground shaking.

Additional evidence for event 2 is suggested by a sand-filled fissure at station +26 m and a thin deposit of the same silty sand (unit 6b) (Fig. 8a) that lies above unit 6c, which is the lateral equivalent to unit 6 in the northern portion of the trench (Fig. 6). The sand-filled fissure is rootless and exhibits sharp margins that narrow abruptly with depth. Because of this geometry, we do not believe that this feature is a krotovina, but rather a fissure from which liquefied silty sand (unit 6b) was ejected onto the paleoground surface (units 6c and 6). This interpretation requires that the fissure deepens out of the plane of the trench wall and is connected to the underlying source of the silty sands by a fracture or pipe. The thin silty sand deposit (unit 6b) is located at about the same stratigraphic position as the upward terminations of the faults (stations −2 to −5 m) that ruptured in event 2 (Fig. 6). Therefore, we prefer to interpret the fissure and silty sand as a liquefaction event associated with event 2.

Finally, it is important to note that we did not observe direct evidence of event 2 along the northwest-striking fault strand at +26 m, along which evidence for event 1 was clear. Thus, it is not clear whether this fault was activated in the penultimate event or whether evidence for an event at that level has simply been obscured by rerupture along the very narrow zone. In either case, as is always possible, other events may have been missed. However, we observed only two liquefaction episodes, each apparently associated with surface faulting, so we believe the record to be complete.

Radiocarbon Dating

One motivation for selecting the Frazier Mountain site was that the closed depression might periodically pond water, creating a favorable environment for peat deposition. Although recent aerial photographs and the presence of both standing water and dried algal mat on the ground indicate that the site does experience ponded water, only a few thin,

discontinuous peatlike layers were exposed in our trenches. Fortunately, abundant detrital charcoal was present throughout the exposed section, and 50 samples were collected for radiocarbon dating from the 1997 portion of the trench alone. Some of the charcoal was associated with *in situ* burn layers and was probably very locally derived, and for this reason, we assume that the charcoal ages approximate the ages of the units in which they are deposited. However, detrital charcoal is always older than the host deposits because time is required to grow and burn the wood prior to its burial in the sediments. Thus, the actual ages of the sediments are probably slightly younger than the radiocarbon ages we reported (Table 2).

Table 2 shows the results for 8 samples of detrital charcoal that were submitted for radiocarbon dating to the University of Arizona. Radiocarbon ages were calibrated to calendric ages using OxCal ver. 3.5 (Ramsey, 1995, 2000), which used the atmospheric data of Stuiver *et al.* (1998) (The 2000 version of the program we used is available online at the following web address: *http://www.rlaha.ox.ac.uk/orau/index.htm*). These samples were chosen from the area nearest the upward termination of the penultimate earthquake (event 2) strands. We chose not to date samples from the uppermost part of the section (units 1–3) because we suspect that they will be younger than 300 years in age and thus be unresolvable due to uncertainties in calibration.

Two of the samples, C-28 (portion of a large piece of wood) and C-21 (an organic peatlike unit) were not detrital charcoal and appear to be inconsistent with results from the other samples dated from the section. Sample C-21 was collected from unit 12, the lowest stratigraphic unit exposed in our trenches. However, it yielded the youngest age of all the samples (Table 2) and may have been contaminated by roots, based on a visual inspection of the sample, thereby yielding an anomalously young age for the sample. Modern roots were visible throughout this unit and, although we removed visible modern roots prior to dating, we suspect that decomposed roots may have significantly contributed to the age of this sample. Alternatively, all of the other samples dated from this section are anomalously old, perhaps due to a residence factor of several hundred years for all of the detrital charcoal samples. Due to the obvious likelihood of contamination of sample C-21, we discard this date and rely on samples of detrital charcoal for age control.

In contrast, sample C-28 yielded the second oldest radiocarbon age of all the samples, and yet it was collected from within Unit 5, which yielded slightly younger sample ages. Thus, we suspect this sample contained significant age at its time of deposition, consistent with the fact that the size of the wood sample required its origin to be from a relatively sizable tree with some time required for growth. For these reasons, samples C-21 and C-28 were not included in the analysis to stratigraphically order the dates using the OxCal program of Ramsey (2000).

Table 2
Dates of Radiocarbon Samples

Stratigraphic Unit	Sample No.	Laboratory No.	Description	$\delta^{13}C$ (%)	^{14}C Age* (Years B.P.)	Calibrated Ages (Calendar Years A.D.)†	Stratigraphically Ordered Dates (Calendar Years A.D.)‡
4	C-41	AA 28795	Detrital charcoal	−25.0§	395 ± 45	1430–1530 A.D. (60.9%) 1540–1640 A.D. (34.5%)	1540–1650 A.D. (95.4%)
5	C-19	AA 28792	Detrital charcoal	−24.6	340 ± 50	1450–1650 A.D. (95.4%) 1300–1370 A.D. (13.7%)	1490–1630 A.D. (95.4%)
5	C-28	AA 9990	Log	−24.7	490 ± 55	1380–1520 A.D. (80.2%) 1600–1620 A.D. (1.5%)	Not included in stratigraphic ordering analysis
5	C-4	AA 28790	Burn layer	−25.2	415 ± 40	1420–1530 A.D. (76.7%) 1560–1630 A.D. (18.7%)	1440–1540 A.D. (94.3%) 1550–1570 A.D. (1.1%)
7	C-12	AA 28791	Detrital charcoal (twig)	−25.0	400 ± 45	1430–1530 A.D. (63.7%) 1540–1640 A.D. (31.7%)	1430–1505 A.D. (95.4%)
7	C-24	AA 28794	Detrital charcoal	−24.3	405 ± 40	1420–1530 A.D. (70.4%) 1550–1640 A.D. (25.0%) 1330–1350 A.D. (1.5%)	1430–1505 A.D. (95.4%)
9	C-3	AA 28789	Detrital charcoal	−24.1	465 ± 45	1390–1520 A.D. (91.6%) 1590–1620 A.D. (2.2%)	1330–1350 A.D. (1.9%) 1390–1470 A.D. (93.5%)
12	C-21	AA 28793	Organic unit with modern roots	−22.8	160 ± 40	1660–1890 A.D. (79.3%) 1910–1960 A.D. (16.1%)	Not included in stratigraphic ordering analysis

*^{13}C corrected ^{14}C age in years B.P. ± 1σ
†Ages calibrated with Oxcal (Ramsey, 2000) using atmospheric data of Stuiver *et al.* (1998); ranges include values within 95.4% confidence limits
‡Stratigraphically ordered ages from Oxcal (Ramsey, 2000)
§$\delta^{13}C$ assumed to be −25.0. because sample was too small for measurement.

The five radiocarbon samples from units above (unit 4), below (unit 7), and within (unit 5) the event 2 event horizon share age ranges, collectively falling between A.D. 1420 and A.D. 1650 (Table 2). In an attempt to refine the age ranges of the radiocarbon samples, and hence, the timing of event 2, we used OxCal (Ramsey, 2000) to reweight the calibrated calendric probability distributions for samples where the age distributions overlap. This methodology of refining layer dates is discussed by Biasi and Weldon (1998) and has been applied to the Wrightwood and Pallett Creek sites along the San Andreas fault (Biasi *et al.*, 2002). We applied a simple stratigraphic ordering constraint to the radiocarbon samples. Since we know that stratigraphically higher layers must be younger than lower layers, we can apply this constraint in OxCal to reweight the calibrated probability distributions. Most often, the result of this constraint is to shift the probability of the multimodal age distribution to one peak. We assume that the sedimentation rate at the site is slow enough on average to expect a true age progression from unit 9 to unit 4 and that applying the stratigraphic ordering of dates is appropriate. The stratigraphically ordered dates resulting from the OxCal analysis are presented in Table 1 and are graphically shown in Figure 9 with their probability distributions and agreement indices. The OxCal program calculates an agreement index, expressed as a percent, for each stratigraphically ordered date that indicates the degree of overlap between the final and initial distribution. The program also calculates an agreement index for the entire sequence of dates, which is 121% (Fig. 9).

The age of the event 1 is constrained by samples collected from below the event horizon. The stratigraphically highest, and therefore, youngest horizon sampled was unit 4 (sample C-41). The stratigraphically ordered age range for this sample is A.D. 1540–1650, which provides a maximum age constraint for event 1. Given that event 1 represents the stratigraphically highest event, we have inferred that this event is the 1857 Fort Tejon earthquake.

The timing of the penultimate event (event 2) is based on bracketing the refined layer dates and leads to an estimate that the event occurred between A.D. 1460 and 1600 (2σ) and is graphically shown in Figure 10. Note that this is an improvement over the simple bracketing of radiocarbon dates, which would have lead to a much less constrained event age of A.D. 1420–1650. The peak of the probability distribution is about A.D. 1510, the most likely age of the event.

It is important to note, however, that this sequencing of dates assumes that sample C-21 derived from the peatlike

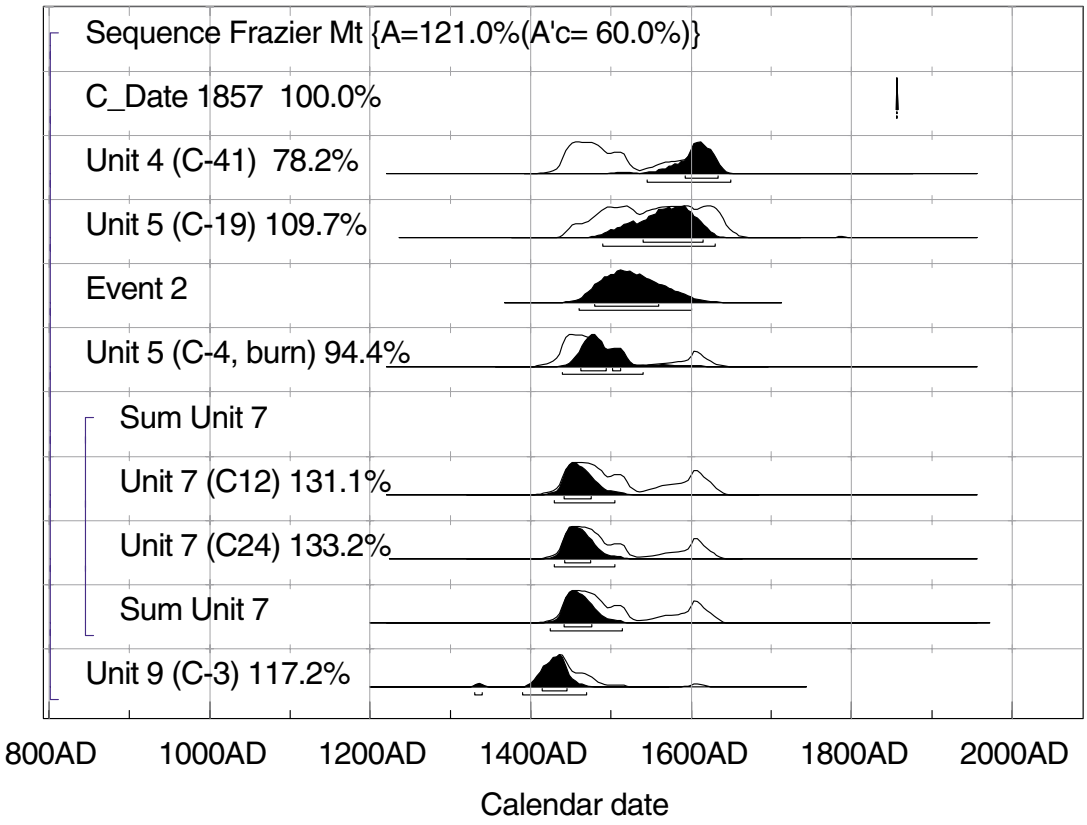

Figure 9. OxCal analysis results of the sequence of radiocarbon dates. Prior calibrated radiocarbon distributions (open curves) and posterior stratigraphically ordered distributions (filled curves) for samples from the Frazier Mountain site. OxCal program Ver. 3.5 (Ramsey, 2000) uses atmospheric data from Stuiver *et al.* (1998).

unit is contaminated with young root carbon. If not, then the entire section may be younger than A.D. 1600, and all of the detrital charcoal samples that we dated have a residence age of 100–200 years. Although we cannot reject this hypothesis without further dating, we consider it unlikely because of the stratigraphic consistency of the other sample ages, the abundance of charcoal in the environment suggesting frequent burns, and the presence of roots in the peat sample. The frequent burn is supported by the observation of *in situ* burn horizons (sample C-4) within the pond sediments. Thus, we conclude that the most likely age for event 2 falls within the period bracketed by the 2σ calibrated age range of A.D. 1460–1600 (Fig. 10).

Discussion

Previous Studies in the Mil Potrero Area

The nearest paleoseismic site to Frazier Mountain is the San Emigdio trench site of Davis (1983), located on the west fork of San Emigdio Creek near the east end of Mil Potrero (Fig. 1). Davis (1983) interpreted evidence for three earthquakes in the last four to five centuries at this site, which lies only 22 km northwest of the Frazier Mountain site. He reported evidence for the 1857 earthquake and two previous events with approximate ages of A.D. 1584 ± 70 (event I) and A.D. 1760 ± 50 (event II). This is in contrast to the results at Frazier Mountain, where we found evidence for only two earthquakes in nearly the same time period. Could event II at San Emigdio Creek represent 1812?

We reviewed the San Emigdio Creek trench log and found it difficult to interpret three events and more likely that the exposure contained stratigraphic evidence for only one and possibly two events. In addition to the significant questions regarding event recognition, there are also considerable limitations in the age dating and the constraints on the timing of events. For instance, single dates were obtained from composite samples of detrital charcoal fragments, two sample ages were combined to obtain an age for event I, and the age of event II is constrained with only a single date. Therefore, we are reluctant to correlate events between Frazier Mountain and the San Emigdio Creek site of Davis (1983) but acknowledge this local work for completeness.

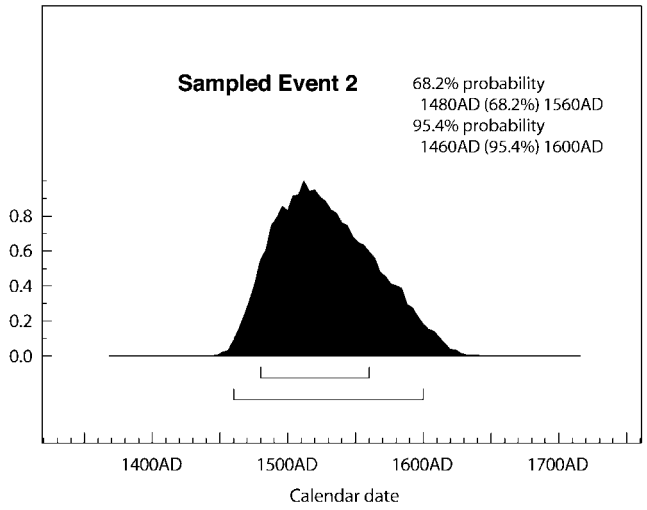

Figure 10. Probability distribution generated by OxCal for the age range of event 2 at Frazier Mountain. The 2σ age range for event 2 is A.D. 1460–1600.

Studies of tree ring growth have also been performed in the Mil Potrero and Cuddy Valley areas and Wrightwood in an attempt to recognize and date previous earthquakes in trees located along the fault (Meisling and Sieh, 1980; Jacoby *et al.*, 1988). Meisling and Sieh (1980) reported that the Whitiner Tree, a Ponderosa pine located about 1.5 km east of the San Emigdio Creek trench site, was severely damaged in the 1857 earthquake, as evidenced by a sudden anomalous reduction in growth rate beginning with the 1857 growing season. The tree, which they estimate reached 1.5 m in height by the 1590s, is over 400 years old and situated 3 m south of the 1857 fault scarp. Jacoby *et al.* (1988) noted that the tree ring data of the Whitiner tree (Meisling and Sieh, 1980) displayed no evidence of disturbance or trauma in 1812, unlike many other trees in the Wrightwood area that record the 1812 event. This led Jacoby *et al.* (1988) to conclude that the 8 December 1812 earthquake did not rupture northwest of Mil Potrero. To the southwest, evidence for the 1812 rupture has been documented at Wrightwood with tree-ring data (Jacoby *et al.*, 1988) and trenching studies (Fumal *et al.*, 1993). At Pallett Creek, Event X was assigned to the 8 December 1812 earthquake by Sieh *et al.* (1989), given the two age ranges (A.D. 1675–1701 or A.D. 1753–1817) for this event (Sieh *et al.*, 1989).

Reinterpretation of historical damage reports has led Toppozada *et al.* (2002) to suggest that the 21 December 1812 earthquake, which was assumed to be centered in the Santa Barbara Channel region (Toppozada *et al.*, 1981), was produced by the San Andreas fault. The new interpretation depicts two San Andreas earthquakes, separated by 13 days, rupturing a ~180- to 200-km section of the fault between the San Bernardino Mountains on the southeast and near Tejon Pass on the northwest. Toppozada *et al.* (2002) suggested that the northwestern half of this segment may be the result of the 21 December event. Future studies in the Tejon Pass area and northern Mojave segment of the fault will hopefully resolve more definitively the extent of 1812 rupture and whether the December 21 event was on the San Andreas fault.

Age of Event 1: 1857 or 1812?

Within the trench exposures at Frazier Mountain, the only two events recognized are events 1 and 2. The age range of A.D. 1460–1600 for event 2 is constrained by radiocarbon dates from above and below the event horizon. However, the age of the younger event 1, which we prefer to assign as the 1857 earthquake, is not constrained by radiocarbon dates. Therefore, a discussion of whether event 1 represents a rup-

ture in 1857 or 1812 is warranted. We tentatively interpret event 1 to represent the 1857 earthquake because (1) it is the highest earthquake observed in the Frazier Mountain stratigraphic section exposed, (2) the event horizon lies only ~50 cm below the present ground surface, and (3) large-slip earthquakes, such as 1857, are more likely to produce complex rupture patterns that involve more strands than smaller, more moderate-sized earthquakes, such as 1812.

Between faults exposed in the trench we can trace continuous, unfaulted stratigraphy both above and below the event 2 horizon, and therefore, we do not observe evidence of an earthquake between the event 1 horizon and the A.D. 1460–1600 horizon (event 2). Furthermore, liquefaction features observed in the trench are only associated with each of the two recognized event horizons and we did not find evidence of liquefaction elsewhere in the stratigraphic section. Thus, we infer that the 1812 earthquake did not rupture as far north as Frazier Mountain. However, our data does not preclude an 1812 event at the site. As shown in Figure 11, we present three possible interpretations for the presence of the two historic earthquakes at our site. In the first scenario, the 1812 event did not occur at Frazier Mountain (scenario 1, Fig. 11). In the second scenario, the 1812 earthquake ruptured through the site, but we were unable to recognize it (scenario 2, Fig. 11). Possible explanations for why 1812 slip may have escaped detection include the following: (1) the amount of slip was very small, (2) the slip occurred on fault strands beyond our trench exposures, or (3) no deposition occurred between 1812 and 1857. In a third scenario, event 1 exposed in the trench at station +26 m (location A in scenario 3, Fig. 11) represents the 1812 event and not 1857 Fort Tejon earthquake. This interpretation would require that (1) all of the ~6 m of slip in 1857 was confined to the northern strand or the more speculative southern strand and (2) no slip occurred on the significant northwest-striking fault that forms a groundwater barrier.

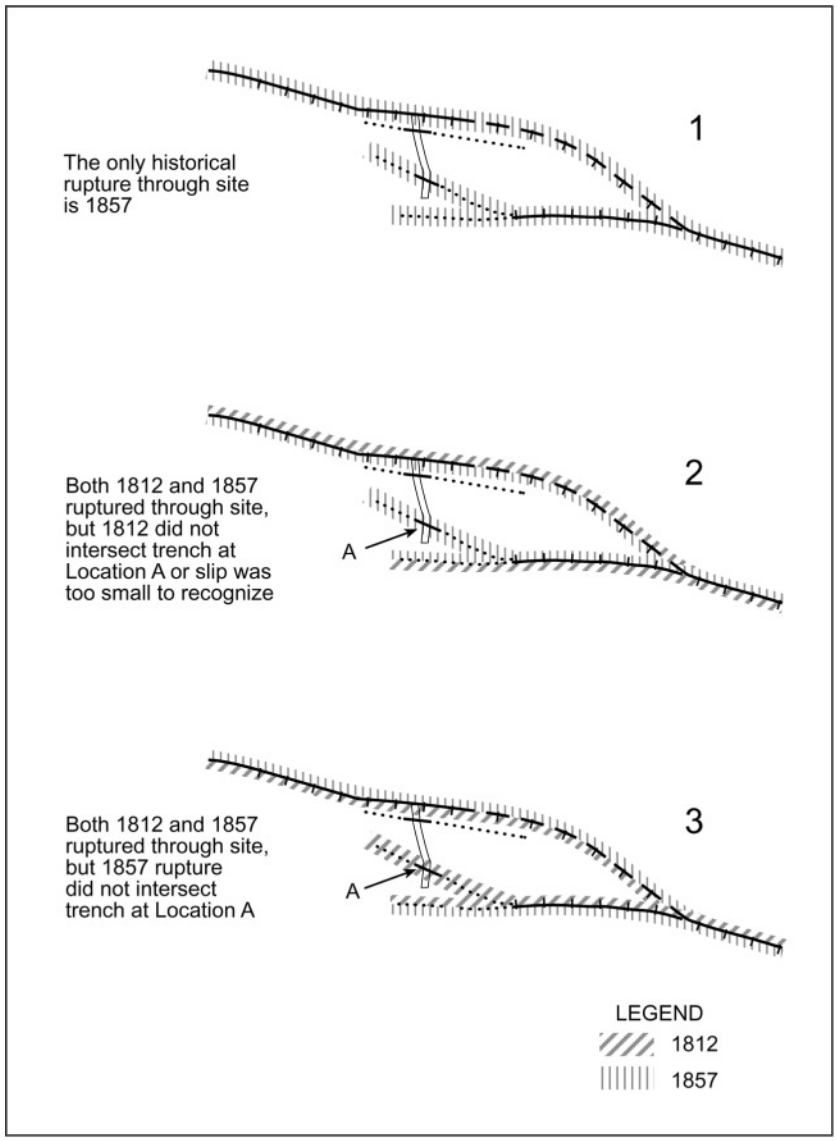

Figure 11. Three scenarios illustrating possible interpretations of the most recent rupture, event 1, at station +26 m (location A) in the trench (open rectangle). In scenario 1, the only historical rupture through the site is the 1857 event. In scenario 2, both the 1812 and 1857 events rupture through the site, however, the 1812 rupture is not recognized in our trench because slip was so minor or it occurred on strands beyond the trench. In scenario 3, event 1 represents the 1812 earthquake. Scenario 3, which we consider the most unlikely interpretation, requires that the smaller 1812 event ruptured the northwest-striking fault at location A and the larger 1857 earthquake did not rupture this strand.

We regard scenario 1 as the most likely interpretation for historical ruptures at Frazier Mountain and scenario 3 as the least likely interpretation (Fig. 11).

Correlation of Event 2 to Other Sites

The correlation of earthquake events between sites is always complicated by both the precision and accuracy of age data at each site. This is particularly the case along the San Andreas fault, where some sites produce high-precision radiocarbon dates on peat deposits and others rely on dating of individual pieces of detrital charcoal. Further, pretreatment of peat samples has changed over the past 20 years, thereby bringing to question the reliability in comparing age results from samples that were treated by different methods (Seitz, 1999). Thus, in the following discussion, it should be understood that we may be able to suggest correlations from one site to another or to discount the possibility that one event is present at another site, but we cannot state categorically that an event at one site is the same as at another site just because their event ages overlap.

Based on the radiocarbon dates obtained in our study, and assuming that sample C-21 is contaminated by roots, as appears to be the case, the penultimate event at the Frazier Mountain site dates to about A.D. 1510 (1460–1600). Considering the errors associated with this age estimate, this event may correlate with a similar aged event at the Bidart site located ~90 km to the northwest in the Carrizo Plain, as well as event V at Pallett Creek located ~105 km to the southeast. Grant and Sieh (1994) constrained the age of the penultimate event at Bidart to be in the range of A.D. 1405–1510 or younger, based on a single radiocarbon age on a grasslike substance. The minor paleosol that was capped by the grass blades is below the event horizon, so the event could conceivably be several decades younger than the reported age. Sieh *et al.* (1989) redated event V at Pallett Creek to A.D. 1465–1495. However, Biasi *et al.* (2002) recalculated the Sieh *et al.* (1989) age range using Baysian layer date constraints to be A.D. 1486–1597 with a preferred event age of 1546. In any case, both event ages are consistent with the age range of Frazier Mountain event 2 (Fig. 12). Event 2 at Frazier Mountain also appears to correlate with the Biasi *et al.* (2002) A.D. 1508–1569 date range of event W4 at Wrightwood (Fig. 12). Similar event dates at other sites southwest of Cajon Pass (Pitman Canyon and Thousand Palms) suggest that the event 2 rupture at Frazier Mountain (if equivalent to events V and W4) may have extended beyond the southern extent of the 1857 event (Seitz *et al.*, 1997; Fumal *et al.*, 2002).

These new data at Frazier Mountain support the idea that the San Andreas fault may have failed in prior 1857-type or larger earthquakes (Grant and Sieh, 1994). Given this similarity and the repeatability of slip (~7–9 m) for the past several ruptures in the Carrizo Plain (Grant and Sieh, 1993), the Fort Tejon earthquake may represent the recent preferred mode of failure for the Carrizo Plain, Big Bend, and Mojave portions of the fault. However, if the San Andreas fault failed with adjacent segment ruptures closely spaced in time, similar to the earthquakes on the North Anatolian fault in August and November of 1999, then these types of events will be interpreted as one large event in the paleoseismic record.

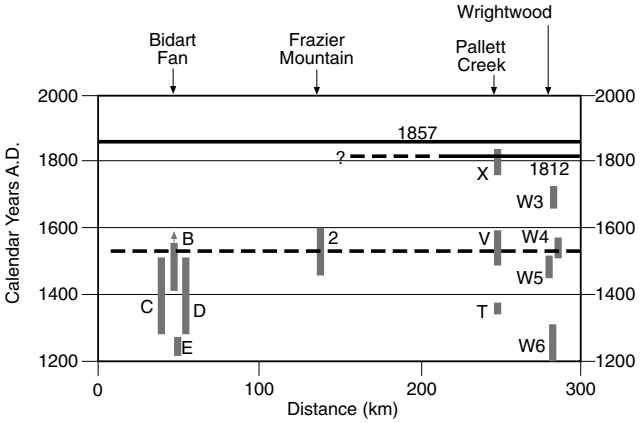

Figure 12. Diagram illustrating probable correlation of Event 2 at Frazier Mountain with similarly dated events at the Bidart Fan, Pallett Creek, and Wrightwood sites. Gray vertical bars represent 2σ age ranges for earthquakes at Bidart fan reported by Grant and Sieh (1994) and for Pallett Creek and Wrightwood reported by Biasi *et al.* (2002). Historic earthquake correlations for the 1857 and 1812 earthquakes are shown as horizontal lines. Event 2 at Frazier Mountain appears to correlate with event B at the Bidart fan site to the northwest and events V and W4 at the Pallett Creek and Wrightwood sites, respectively, to the southeast.

Acknowledgments

We would like to thank Arley and Michael Beane of Mesa Valley Farms for granting us access to their property to perform these studies. We are grateful for their patience and appreciate their willingness to allow us to conduct our studies, especially in this current climate when access to private land is becoming increasingly difficult for researchers. We are indebted to Christopher Hitchcock and Carrie Randolph for their long days of surveying with the total station to create a detailed topographic map of the site. Discussions with Tousson Toppozada and reviews of the manuscript from Jeri Young and an anonymous reviewer led to significant improvements. This research was supported by the Southern California Earthquake Center (SCEC). SCEC is funded by National Science Foundation cooperative agreement EAR-8920136 and U.S. Geological Survey Cooperative Agreement 14-08-001-A0899 and 1434-HQ-97AG01718. The SCEC Contribution Number for this article is 599.

References

Biasi, G., and R. J. Weldon (1998). Paleoseismic date refinement and implications for seismic hazard estimation, in *Dating and Earthquakes: Review of Quaternary Geochronology and Its Application to Paleoseismology*, J. M. Sowers, J. S. Noller, and W. R. Lettis (Editors), NUREG/CR-5562, U.S. Nuclear Regulatory Commission, 3-61–3-66.

Biasi, G., R. Weldon, T. Fumal, and G. Seitz (2002). Paleoseismic event dating and the conditional probability of large earthquakes on the

southern San Andreas fault, California, *Bull. Seism. Soc. Am.* **92,** no. 7, 2761–2781.

Crowell, J. C. (1952). Geology of the Lebec Quadrangle, *Calif. Div. Mines Geol. Spec. Rept. 24*, 23 pp.

Davis, T. L. (1983). Late Cenozoic structure and tectonic history of the western "Big Bend" of the San Andreas fault and adjacent San Emigdio Mountains, *Ph.D. Thesis*, University of California, Santa Barbara, 578 pp.

Duebendorfer, E. M. (1979). Geology of the Frazier Park-Cuddy Valley area, California, *M.A. Thesis*, University of California, Santa Barbara, 123 pp.

Fumal, T. E., S. K. Pezzopane, R. J. Weldon II, and D. P. Schwartz (1993). A 100-year average recurrence interval for the San Andreas fault at Wrightwood, California, *Science* **259,** 199–203.

Fumal, T. E., M. J. Rymer, and G. G. Seitz (2002). Timing of large earthquakes since A.D. 800 on the Mission Creek Strand of the San Andreas fault zone at Thousand Palms Oasis, near Palm Springs, California, *Bull. Seism. Soc. Am.* **92,** no. 7, 2841–2860.

Grant, L. B., and K. Sieh (1993). Stratigraphic evidence for seven meters of dextral slip on the San Andreas fault during the 1857 earthquake in the Carrizo Plain, *Bull. Seism. Soc. Am.* **83,** 619–635.

Grant, L. B., and K. Sieh (1994). Paleoseismic evidence of clustered earthquakes on the San Andreas fault in Carrizo Plain, California, *J. Geophys. Res.* **99,** 6819–6841.

Jacoby, G., P. Sheppard, and K. Sieh (1988). Irregular recurrence of large earthquakes along the San Andreas fault: evidence from trees, *Science* **241,** 196–198.

Meisling, K. E., and K. E. Sieh (1980). Disturbance of trees by the 1857 Fort Tejon earthquake, California, *J. Geophys. Res.* **85,** 3225–3238.

Ramsey, B. C. (1995). Radiocarbon calibration and analysis of stratigraphy: the OxCal program, *Radiocarbon* **37,** 425–430.

Ramsey, B. C. (2000). Online version of the OxCal program, Ver. 3.5, Oxford Radiocarbon Accelerator Unit, *http://www.rlaha.ox.ac.uk/orau/index.htm* (last accessed 30 May 2001).

Seitz, G. (1999). The Paleoseismology of the San Andreas fault at Pitman Canyon, implications for fault behavior and paleoseismic methodology, *P.h.D. Thesis*, University of Oregon, Eugene, Oregon.

Seitz, G., R. J. Weldon, and G. P. Biasi (1997). The Pitman Canyon paleoseismic record: a reevaluation of southern San Andreas fault segmentation, *J. Geodynam.* **24,** no. 1–4, 129–138.

Sieh, K. E. (1978). Slip along the San Andreas fault associated with the great 1857 earthquake, *Bull. Seism. Soc. Am.* **68,** 1421–1448.

Sieh, K. E. (1996). The repetition of large-earthquake ruptures, *Proc. Natl. Acad. Sci.* **93,** 3764–3771.

Sieh, K. E., and R. H. Jahns (1984). Holocene activity of the San Andreas fault at Wallace Creek, California, *Geol. Soc. Am. Bull.* **95,** 883–896.

Sieh, K. E., M. Stuiver, and D. Brillinger (1989). A more precise chronology of earthquakes produced by the San Andreas fault in southern California, *J. Geophys. Res.* **94,** 603–623.

Stuiver M., P. J. Reimer, E. Bard, J. W. Beck, G. S. Burr, K. A. Hughen, B. Kromer, F. G. McCormac, J. von der Plicht, and M. Spurk (1998). INTCAL98 Radiocarbon age calibration 24,000–0 BP, *Radiocarbon* **40,** 1041–1083.

Toppozada, T., D. Branum, M. Reichle, C. Hallstrom (2002). San Andreas fault, California, $M \geq 5.5$ earthquakes 1800–2001, *Bull. Seism. Soc. Am.* **92,** no. 7, 2555–2601.

Toppozada, T. R., C. R. Real, and D. L. Parke (1981). Preparation of isoseismal maps and summaries of reported efforts for pre-1900 California earthquakes, Annual Technical Report to U.S. Geol. Surv., *Calif. Div. Mines Geol. Open-File Rept. 81-11SAC*, 182 pp.

Zhou, X., E. A. Keller, and D. L. Johnson (1991). Tectonic geomorphology of the Frazier Mountain area, in *Active Folding and Reverse Faulting in the Western Transverse Ranges, Southern California*, E. A. Keller (Editor), Field Trip Guidebook, Geol. Soc. Am. Annual Meeting, Geological Society of America, 50–60.

William Lettis & Associates, Inc.
28470 Avenue Stanford, Suite 120
Valencia, California 91355
(S.C.L., J.G.H., K.W.B.)

Department of Geological Sciences
San Diego State University
San Diego, California 92182
(T.K.R.)

U.S. Geological Survey
345 Middlefield Road, MS 977
Menlo Park, California 94025
(T.E.D.)

Manuscript received 2 July 2001.